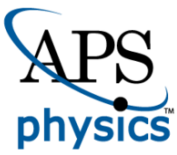

Chirality Waves in Two-Dimensional Magnets

D. Solenov, D. Mozyrsky, and I. Martin

Phys. Rev. Lett. **108**, 096403 — Published 29 February 2012

DOI: 10.1103/PhysRevLett.108.096403

Chirality waves in two-dimensional magnets

D. Solenov, D. Mozyrsky, and I. Martin
Theoretical Division, Los Alamos National Laboratory, Los Alamos, NM 87545, USA

We theoretically show that moderate interaction between electrons confined to move in a plane and localized magnetic moments leads to formation of a noncoplanar magnetic state. The state is similar to the skyrmion crystal recently observed in cubic systems with the Dzyaloshinskii-Moriya interaction; however, it does not require spin-orbit interaction. The non-coplanar magnetism is accompanied by the ground-state electrical and spin currents, generated via the real-space Berry phase mechanism. We examine the stability of the state with respect to lattice discreteness effects and the magnitude of magnetic exchange interaction. The state can be realized in a number of transition metal and magnetic semiconductor systems.

PACS numbers:

Magnetism is a cooperative phenomenon where spins of magnetic ions spontaneously orient relative to each other below certain ordering temperature [1, 2]. In principle, arbitrarily complex magnetic orderings are possible; however, the magnetic states encountered in nature tend to be simple, the most common being ferromagnetism (one atom in magnetic unit cell, Fig. 1a) and antiferromagnetism (two distinct atoms in magnetic unit cell, Fig. 1b). More complex orders [3–6], such as noncollinear spirals (Fig. 1d) and various noncoplanar orders (e.g., Fig. 1e) are less common, typically arising from the interplay of magnetic exchange interactions, spin-orbit (SO) coupling [5], frustrated lattice structure [3], and magnetic field [6].

Noncoplanar magnetism has a unique effect on electronic transport through coherently influencing the quantum-mechanical phase of electrons [7]. The phase accumulates when an electron moves through the magnetic texture and adjusts its spin according to the local magnetic environment. The resulting Berry phase is equal to half of the solid angle subtended by electron spin in the process of its evolution around a closed trajectory (Fig. 1c). This is similar to the Aharonov-Bohm phase induced by the electromagnetic vector potential which couples to electron charge. If the magnetic texture varies significantly on the scale of the material unit cell, the equivalent magnetic field strength can be gigantic, exceeding 10^4 Tesla. Consequently, in non-coplanar magnets one may find such exotic magneto-transport phenomena as the intrinsic anomalous Hall effect [8], Hall effect in the absence of net magnetization or magnetic field [9], or even quantum anomalous Hall effect [10, 11].

In the absence of SO coupling or magnetic field, the non-coplanar states have been believed to be very rare [12, 13]. Recently, however, several examples have been found that show energetic preference for non-coplanar magnetic states [11, 14–17] in one of the simplest models of magnetism – the isotropic Kondo lattice model – even in the absence of SO interaction. These noncoplanar states were found for particular lattice structures and electron densities, which leaves an open question: How common are the non-coplanar magnetic states? Here, we show that non-coplanar magnetic states occur in the low-density regime of 2D Kondo lattice models without fine tuning. Our numerical results suggest that in the weak-to-moderate coupling regime, the lowest energy state is a "skyrmion crystal" [18], with the spatial period determined by the Fermi wavelength, $\lambda_F \sim 1/q_F$. The texture $\mathbf{S}(\mathbf{r})$ can be characterized by the scalar spin chirality density, $\kappa = \mathbf{S}\cdot[\partial_x\mathbf{S}\times\partial_y\mathbf{S}]$, which measures the density of the Berry phase ("Berry curvature"), and hence is related to the effective orbital magnetic field acting on electrons. We find that κ is spatially modulated, leading to persistent bulk electrical and spin currents within the ground state.

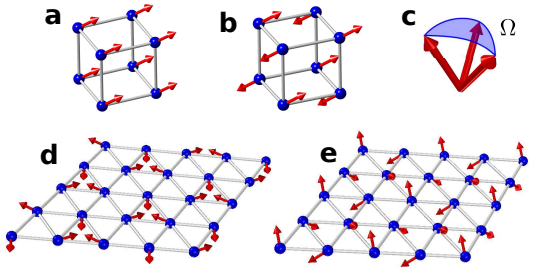

FIG. 1: Types of magnetic ordering. Collinear magnetic states: (a) ferromagnet and (b) antiferromagnet. (d) Non-collinear (but coplanar) magnetic spiral state. (e) Example of *non-coplanar* magnetic state, from Ref. [11]. (c) Solid angle Ω subtended by three local moments forming an elementary plaquette of a triangular lattice induces a quantum Berry phase $\pm\Omega/2$ for electrons circling the plaquette, locally aligned/antialigned with the texture.

The starting point of our analysis is the continuum limit of the Kondo lattice model, which describes itinerant electrons interacting with localized moments,

$$\mathcal{H} = -\Psi^\dagger\frac{\hbar^2\partial_{\mathbf{r}}^2}{2m}\Psi - J\mathbf{S}(\mathbf{r})\cdot\Psi^\dagger\boldsymbol{\sigma}\Psi \equiv \Psi^\dagger\hat{H}\Psi. \qquad (1)$$

Here $\Psi = [\psi_\uparrow(\mathbf{r}), \psi_\downarrow(\mathbf{r})]^T$ is the itinerant electron field operator, m is the electron mass, $\boldsymbol{\sigma} = (\sigma_x, \sigma_y, \sigma_z)$ is vector of the Pauli matrices and $\mathbf{S}(\mathbf{r})$ is the spin of the mag-

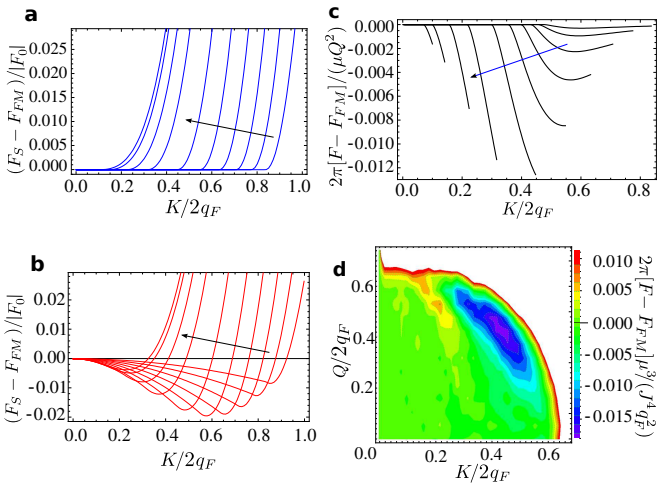

FIG. 2: Instability of coplanar spiral state. (a,b) Free energy of the spiral state $\mathbf{S}(\mathbf{r}) = (\sin Ky, 0, \cos Ky)$ with the ordering vector K for the Kondo coupling values $J/\mu = 0.3, 0.4, 0.5, 0.6, 0.7, 0.8, 0.9, 0.95, 0.98, 0.99$ (arrows indicate the direction of increasing J/μ). (a) Exact degeneracy of all spiral states with $K < 2q_F\sqrt{1 - J/\mu}$. (b) Lifting of the degeneracy in favor of $K \neq 0$ states due to non-parabolicity of the electron band. Here, the quartic terms in the dispersion have been introduced to replicate the effect of the finite electron bandwidth, $\mu/t = 0.24$, with t the nearest neighbor hopping on a square lattice. (c,d) Energy of the non-coplanar variational *ansatz* $\tilde{\mathbf{S}}(\mathbf{r}) = (\sin Ky \cos Qx, \sin Ky \sin Qx, \cos Ky)$. (c) Semi-analytical result of the small-Q expansion for the scaled energy difference $2\pi[F(K,Q) - F_{FM}]/(\mu Q^2)$, obtained in the continuum limit (J/μ increases from right to left curves as before). The difference becomes negative in some range of values $K_0 < K < 2q_F\sqrt{1 - J/\mu}$, indicating energetic preference for states with $Q \neq 0$. (d) Free energy of the same *ansatz* for arbitrary values of Q obtained by direct numerical diagonalization of the Hamiltonian with $J/\mu = 0.67$.

netic atom located at $\mathbf{r}$. The local magnetic moments may originate from the electrons partially occupying d- or f-core levels, whose spins are aligned by the ferromagnetic Hund's interaction. When their combined angular momentum is large, the behavior of $\mathbf{S}(\mathbf{r})$ becomes nearly classical, i.e., slow compared to itinerant electrons. From the stand point of itinerant electrons the problem then becomes tractable, since the Hamiltonian is quadratic in electron fields and therefore can be exactly numerically diagonalized for an arbitrary static configuration of the classical moments $\mathbf{S}(\mathbf{r})$. The sign of the Kondo coupling J does not matter in the case of classical local moments, so we take $J > 0$.

The simplest approach to look for the ordered states in the Kondo lattice model is by integrating out the electronic degrees of freedom perturbatively in J. In the lowest (2nd) order in J, the result is the classical Heisenberg Hamiltonian [19],

$$H_{RKKY} = -J^2 \sum\nolimits_{i,j} \chi(\mathbf{r}_i - \mathbf{r}_j)\, \mathbf{S}_i \cdot \mathbf{S}_j, \qquad (2)$$

that describes a system of local moments coupled by pair-wise interactions. The spatial dependence of the interaction is determined by the non-interacting electron spin susceptibility $\chi(\mathbf{r})$. Due to translational invariance, the ground state of this approximate model can be easily found by transforming to the Fourier space [20], $H_{RKKY} = -J^2 \sum_{\mathbf{q}} \chi(\mathbf{q})\, \mathbf{S}_{-\mathbf{q}} \cdot \mathbf{S}_{\mathbf{q}}$. From the fixed length (classical) constraint, $|\mathbf{S}_i| = 1$, it follows that $\sum_{\mathbf{q}} \mathbf{S}_{-\mathbf{q}} \cdot \mathbf{S}_{\mathbf{q}} = N$, where N is the number of magnetic atoms in the system. Therefore, the energy H_{RKKY} is minimized by, e.g., a simple spiral state with the wave vector $\mathbf{q_0}$ that maximizes the non-interacting electron spin susceptibility $\chi(\mathbf{q})$. The momentum dependence of the susceptibility is determined by the itinerant electron band structure. In particular, in one-dimensional (1D) systems susceptibility diverges at twice the Fermi momentum, and hence $q_0 = 2q_F$; in 2D continuum (low electron density) limit it is flat up to $2q_F$, which makes all states with $q < 2q_F$ energetically equivalent; in 3D continuum $\mathbf{q}_0 = 0$, which corresponds to ferromagnetism. A distortion of the Fermi surface (and in particular "nesting") due to lattice discreteness effects can enhance susceptibility at a non-trivial $\mathbf{q}_0$, even in 3D. The main limitation of the approach based on the quadratic Hamiltonian H_{RKKY} is that it does not energetically discriminate between the single-$\mathbf{q}_0$ coplanar or multiple-$\mathbf{q}_0$ non-coplanar orderings, as long as the constraint $|\mathbf{S}_i| = 1$ is satisfied [21]. Hence the simple description provided by H_{RKKY}, while useful in determining the optimal ordering vectors in the weak-coupling regime, is inadequate to answer the main question of this Letter: When does the Kondo lattice model support non-coplanar magnetic states?

To address this question we need to more accurately compare the energy of non-coplanar magnetic states with the simpler candidates for the ground state ordering in the Kondo lattice model: the ferromagnetic and the coplanar spiral states. We will focus on the low-density 2D systems because they are expected to be particularly prone to complex orderings, due to the massive degeneracy within the J^2-order description (2). In the ferromagnetic state, the free energy density at zero temperature can be analytically evaluated as $F_{FM} = F_0(1 + J^2/\mu^2)$ when $J < \mu$ and $F_{FM} = \frac{1}{2}F_0(1 + J/\mu)^2$ when $J > \mu$, where $F_0 = -(m/2\pi\hbar^2)\mu^2$ is the energy of the non-interacting electron gas with effective mass m and chemical potential $\mu = \hbar^2 q_F^2/2m$. The stability of the ferromagnetic state for $J > \mu$ follows from the gradient expansion of the free energy,

$$F - F_{FM} = \Theta(J^2 - \mu^2)\frac{J^2 - \mu^2}{8\pi J}\int \frac{d\mathbf{r}}{V}|\nabla \mathbf{S}|^2, \qquad (3)$$

where $\Theta(x)$ is the Heaviside step function and V is the volume of the system. For values of $J < \mu$, ferromagnet loses stiffness. Remarkably, in this regime, the ferromagnetic state is *exactly* degenerate (to all orders in J) with

all spiral states, $\mathbf{S}(\mathbf{r}) = (\sin Ky, 0, \cos Ky)$,

$$F_S = \sum_{\pm} \int \frac{d\mathbf{q}}{(2\pi\hbar)^2} [\varepsilon_{\pm}(\mathbf{q}) - \mu]\Theta(\mu - \varepsilon_{\pm}(\mathbf{q})), \qquad (4)$$

$$\varepsilon_{\pm}(\mathbf{q}) = \frac{\hbar^2 q^2}{2m} + \frac{\hbar^2 K^2}{8m} \pm \sqrt{\frac{\hbar^4 K^2 q_y^2}{4m^2} + J^2}, \qquad (5)$$

as long as $K \leq 2q_F\sqrt{1 - J/\mu}$, see Fig. 2a. This degeneracy is lifted when deviations from parabolic dispersion are included. For instance, for low-density electrons hopping between nearest neighbor sites on a square lattice, there is an energetic preference towards a spiral with $K \approx 2q_F\sqrt{1 - J/\mu}$, Fig. 2b.

To determine whether the simple spiral states are unstable with respect to non-coplanar distortions, we introduce a slow modulation in the texture with the wave vector Q perpendicular to K, $\tilde{\mathbf{S}}(\mathbf{r}) = (\sin Ky \cos Qx, \sin Ky \sin Qx, \cos Ky)$. The free energy correction due to finite Q can be obtained by local spin rotation of the Hamiltonian (1) to

$$\hat{H}' = \frac{\hbar^2 q_x^2}{2m} - \frac{\hbar^2 \partial_y^2}{2m} + \frac{\hbar^2 K^2}{8m} + \frac{\hbar^2 K i \partial_y}{2m}\sigma_y - J\sigma_z + \frac{\hbar^2 Q^2}{8m} - \frac{\hbar^2 Q q_x}{2m}(\sigma_z \cos Ky - \sigma_x \sin Ky), \qquad (6)$$

and subsequent expansion to the second order in Q, which yelds

$$F' = F_{FM} + [Q^2\mu/8\pi][1 + I(K)] + \mathcal{O}(Q^4) \qquad (7)$$

$$I(K) = \int_{-\infty}^{\infty} dx dy \int_C dz \frac{x^2 \prod_{\pm}\left[z - 2\frac{K}{q_F}\left(y \pm \frac{K}{2q_F}\right)\right]}{\pi^2 \prod_{\pm}\left\{z\left[z - 2\frac{K}{q_F}\left(y \pm \frac{K}{2q_F}\right)\right] - \frac{J^2}{\mu^2}\right\}}. \qquad (8)$$

The integration over z is to be performed along the line $\mathrm{Re}(z) = x^2 + y^2 - 1$. The integrals over z and x can be evaluated analytically, while the final integral over y is computed numerically. The result is presented in Fig. 2c. Notably, for small K, the Q^2 correction is identically zero. At some finite momentum $K_0 < 2q_F\sqrt{1 - J/\mu}$, however, the correction becomes negative. This proves unambiguously that any simple spiral (as well as ferromagnetic) state in the continuum limit of the Kondo lattice model has higher energy than a more complex non-coplanar magnetic state for $J < \mu$. Direct numerical evaluation of the free energy can also be performed for arbitrary values of Q and K, by exact diagonalization of the Hamiltonian (6), Fig. 2d. For $J \ll \mu$, the minimum is reached by a noncoplanar state $\tilde{\mathbf{S}}(\mathbf{r})$ with $Q \approx K \approx q_F$. The energetic advantage scales as $\mathcal{O}(J^4)$, which is naturally outside the accuracy of the description provided by H_{RKKY}.

A distinctive feature of state $\tilde{S}(\mathbf{r})$ is the harmonically modulated scalar spin chirality, $\kappa \propto \sin(Ky)$ (Fig. 3e),

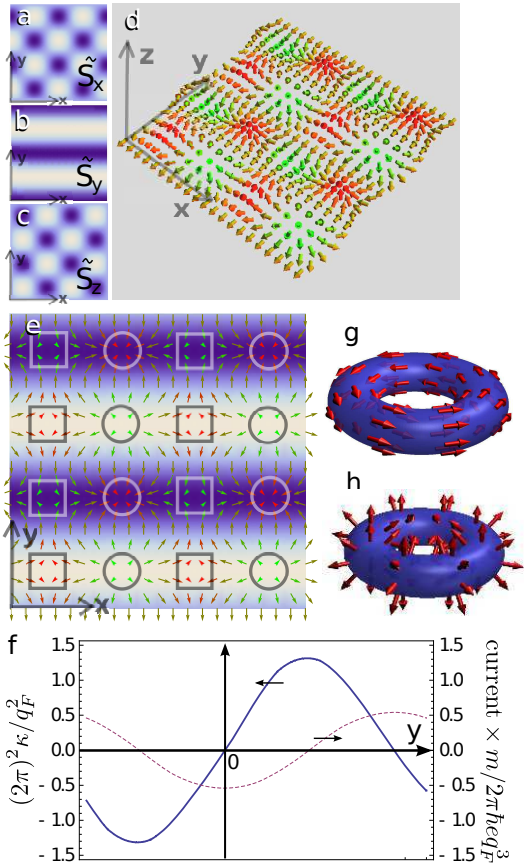

FIG. 3: (a-e) The optimal magnetic state $\tilde{\mathbf{S}}(\mathbf{r}) = (\sin Ky \cos Kx, -\cos Ky, \sin Ky \sin Kx)$ realized at small Kondo coupling, $J/\mu \ll 1$. Panels (a-c) show the spatial dependence of the three magnetization components. (d) Full 3D magnetization pattern. (e) The in-plane magnetization has a "vortex-antivortex" structure (vortex points are marked with circles, antivortex points — with squares). The color of the arrows (green/red) represents the direction (down/up) of the S_z component of the local moments. The superimposed density plot in **e** represents scalar chirality, $\kappa = \mathbf{S}\cdot[\partial_x\mathbf{S} \times \partial_y\mathbf{S}]$. (f) 1D cut showing the chirality density and the induced charge current density in the lowest energy state, $\tilde{\mathbf{S}}(\mathbf{r})$, for $J = 0.2$ and $\mu = 0.5$. (g,h) The two-dimensional periodic magnetization patterns can be naturally mapped onto toroidal surface representing the real space magnetic unit cell. A simple spiral texture, (g), is unstable with respect to configuration (h) that corresponds to the $\tilde{\mathbf{S}}(\mathbf{r})$ texture.

which plays a role analogous to a spatially varying magnetic field perpendicular to the plane of the sample. Due to the effective spin-dependent Lorentz force acting on electrons, there are both spin and charge Hall effects associated with the local value of κ in the absence of an externally applied magnetic field [charge Hall effect appears due to the imbalance between electron spin populations aligned and anti-aligned with the local exchange field $J\mathbf{S}(\mathbf{r})$]. In the electron band structure, magnetic ordering leads to opening of multiple energy gaps; however, overall the system remains metallic and hence there

is no quantum Hall effect. Nevertheless, similar to the quantum Hall systems where one obtains persistent edge currents, here we find spontaneous ground state current *in the bulk*, with the maxima of the current magnitude occurring at the nodes of κ, Fig 3f.

We now discuss the possibility of other noncoplanar states. In the limit of small J/μ and very low electron density, there are stringent constraints on the kinds of states that can be the ground state of the Hamiltonian (1). In particular, any Fourier components $\mathbf{S_q}$ that fall outside the circle $q < 2k_F$, would incur energy cost of order J^2. For instance, this rules out the hexagonal skyrmion crystals [18] in this regime, since for classical spins it contains an infinite number of harmonics. On the other hand, for the state $\tilde{\mathbf{S}}(\mathbf{r})$, all Fourier harmonics $\mathbf{S_q}$ can be confined to the circle $q < 2k_F$, making it degenerate with spiral and ferromagnetic states in the J^2 order, but energetically favored in the order J^4. Thus, in the limit $J \ll \mu$, $\mathbf{S_q}$ is a likely candidate for the absolute ground state of the system. The highly symmetric nature of $\tilde{\mathbf{S}}(\mathbf{r})$ can be appreciated by mapping it onto a torus representing the real space magnetic unit cell. It corresponds to the Gauss' map, which associates a normal vector to every point of the torus, Fig. 3h. One can easily see that the map is in the same topological sector as the spiral (Fig. 3g) and the ferromagnetic states (trivial map), as they can be smoothly distorted into each other without changing the real space unit cell. (This is in contrast to the map that corresponds to the hexagonal skyrmion crystal. It has a wrapping number 1, i.e. the unit sphere of $\mathbf{S}(\mathbf{r})$ is covered exactly once upon integration over the real space unit cell).

At intermediate values of J/μ, the higher-order contributions to energy may become comparable to the second-order (RKKY) terms and the simple perturbative arguments can no longer be applied. In this regime, we speculate that a hexagonal skyrmion crystal may become favorable as it can open more easily a full gap in the electronic spectrum around the Fermi surface for moderate values of J/μ, even though in the order J^2 it loses to $\tilde{\mathbf{S}}(\mathbf{r})$. Similarly, quasicrystalline orders that have even higher order rotational symmetries, e.g. 8- or 10-fold, can become competitive in the intermediate J/μ regime since they can open the gap around the Fermi surface even more effectively. Whether these possibilities are realized in the model (1) is a challenging problem.

Finally, we comment on the effects of lattice discreteness, which causes deviations from the pure parabolic dispersion assumed in the model (1). In Fig. 2b we have seen that the energy of the simple spiral state decreases on a lattice. It is therefore important to analyze how the range of stability of the noncoplanar phase is modified by this effect. By directly evaluating the energy of the spiral vs. non-coplanar state on a square lattice with only nearest neighbor hopping at finite densities we have found that the region of stability of the noncoplanar state behaves as $\kappa\mu < J < \mu$ with $\kappa \approx 0.4$. The value of κ will depend on the type of tight-binding model; the better the dispersion fits the parabolic dispersion of free electrons, the smaller the value of κ. The details, along with the numerical results of the unconstrained energy minimization on finite real-space magnetic unit cells, are presented in the Supplemental material.

Even though our focus has been on the zero-temperature behavior in 2D systems, we expect that the results will remain qualitatively valid in quasi-2D systems up to finite temperatures. Consequently, one can anticipate that non-coplanar magnetism with concomitant exotic Hall behavior, may appear in a wide range of materials and artificial structures, including magnetic monolayers on metallic surfaces [22], layered magnetic materials [23], dilute magnetic semiconductor films [24], and transition metal oxide heterostructures. In particular, recent studies of the Hall conductivity in thin films of Mn doped GaAs show highly unusual behavior, which cannot be explained within the conventional mechanisms of the anomalous Hall effect [24]. The carrier concentrations and the exchange coupling strengths, controlled by the Mn concentration, place this system in the interesting weak-to-intermediate coupling regime considered in this Letter, indicating possible relevance of our consideration to this system.

We thank C. D. Batista, A. Morpurgo, D. Podolsky, R. Wiesendanger, and A. Zheludev for discussions. This work was carried out under the auspices of the National Nuclear Security Administration of the U.S. Department of Energy at Los Alamos National Laboratory under Contract No. DE-AC52-06NA25396 and supported by the LANL/LDRD Program.

[1] P. Grünberg, *et al.*, Phys. Rev. Lett. **57**, 2442 (1986).
[2] M. B. Salamon and M. Jaime, Rev. Mod. Phys. **73**, 583 (2001).
[3] S. T. Bramwell and M. J. P. Gingras, Science **294**, 1495 (2001).
[4] H. B. Braun, *et al.*, Nature Physics **1**, 159 (2005).
[5] M. Bode, *et al.*, Nature **447**, 190 (2007); C. Pappas, *et al.*, Phys. Rev. Lett. **102**, 197202 (2009).
[6] S. Mühlbauer, *et al.*, Science **323**, 915 (2009); X. Z. Yu, *et al.*, Nature **465**, 901 (2010).
[7] J. Ye, *et al.*, Phys. Rev. Lett. **83**, 3737(1999).
[8] Y. Taguchi, *et al.*, Science **291**, 2573 (2001); A. Neubauer, *et al.*, Phys. Rev. Lett. **102**, 186602 (2009).
[9] Y. Machida, *et al.*, Nature **463**, 210 (2009).
[10] K. Ohgushi, S. Murakami, and N. Nagaosa, Phys. Rev. B **62**, R6065 (2000); R. Shindou and N. Nagaosa, Phys. Rev. Lett. **87**, 116801 (2001).
[11] I. Martin and C. D. Batista, Phys. Rev. Lett. **101**, 156402 (2008).
[12] T. Momoi, K. Kubo, and K. Niki, Phys. Rev. Lett. **79**, 2081 (1997).
[13] J.-C. Domenge, *et al.*, Phys. Rev. B **77**, 172413 (2008).

[14] G.-W. Chern, Phys. Rev. Lett. **105**, 226403 (2010).
[15] Y. Akagi and Y. Motome, J. Phys. Soc. Jpn. **79**, 083711 (2010).
[16] Y. Kato, I. Martin, and C. D. Batista, Phys. Rev. Lett. **105**, 266405 (2010) .
[17] S. Kumar and J. van den Brink, Phys. Rev. Lett. **105**, 216405 (2010).
[18] U. K. Rößler, A. N. Bogdanov, and C. Pfleiderer, Nature **442**, 797 (2006).
[19] M. A. Ruderman and C. Kittel, Phys. Rev. **96**, 99 (1954).
[20] J. Villain, J. Phys. (Paris) **38**, 385(1977).
[21] Thermal or quantum fluctuations can eliminate degeneracies of classical spin models. In our case, we show however, that the ground state degeneracy is naturally lifted by the more accurate treatment of the Kondo lattice model, i.e. by going beyond quadratic approximation.
[22] S. Heinze, *et al.*, Nature Physics **7**, 713 (2011).
[23] F. Ronning, *et al.*, Journal of Magnetism and Magnetic Materials **310**, 392 (2007).
[24] D. Chiba, *et al.*, Phys. Rev. Lett. **104**, 106601 (2010).